CONF-8711217--6

CTH: A Three-Dimensional Shock Wave Physics Code*

SAND--89-0607C

DE89 016529

J. Michael McGlaun and S. L. Thompson

Sandia National Laboratories
Albuquerque, New Mexico

M. G. Elrick

Kaman Sciences Corporation
Albuquerque, New Mexico

Abstract

CTH is a software system under development at Sandia National Laboratories Albuquerque to model multidimensional, multi-material, large deformation, strong shock wave physics. One-dimensional rectilinear, cylindrical, and spherical meshes; two-dimensional rectangular, and cylindrical meshes; and three-dimensional rectangular meshes are currently available. A two-step Eulerian solution scheme is used with these meshes. The first step is a Lagrangian step in which the cells distort to follow the material motion. The second step is a remesh step where the distorted cells are mapped back to the Eulerian mesh.

CTH has several models that are useful for simulating strong shock, large deformation events. Both tabular and analytic equations of state are available. CTH can model elastic-plastic behavior, high explosive detonation, fracture, and motion of fragments smaller than a computational cell. The elastic-plastic model is elastic-perfectly plastic with thermal softening. A programmed burn model is available for modelling high explosive detonation. The Jones-Wilkins-Lee equation of state is available for modelling high explosive reaction products. Fracture can be initiated based on pressure or principle stress. A special model is available for moving fragments smaller than a computational cell with statistically the correct velocity. This model is very useful for analyzing fragmentation experiments and experiments with witness plates.

CTH has been carefully designed to minimize the dispersion present in Eulerian codes. It has a high-resolution interface tracker that prevents breakup and distortion of material interfaces. It uses second order convection schemes to flux all quantities between cells.

This paper describes the models, and novel features of CTH. Special emphasis will

*This work performed at Sandia National Laboratories supported by the U.S. DOE under contract DE-AC04-76DP00789.

---

be placed on the features that are novel to CTH or are not direct generalizations of two-dimensional models. Another paper by Trucano and McGlaun [1] describes several hypervelocity impact calculations using CTH.

Introduction

The CTH system allows the analyst to set up and examine the initial configuration, integrate the problem through time, and examine the results with one integrated software family. The current version of CTH uses an Eulerian treatment where the mesh is fixed in space and the material flows through the mesh.

Six geometry options are available in CTH: one-dimensional rectangular, cylindrical, and spherical geometries; two-dimensional rectangular and cylindrical geometries; and three-dimensional rectangular geometry. Up to ten materials and void can occupy a computational cell.

The conservation equations are replaced by finite volume approximations. The finite volume approximations have been carefully designed to conserve mass, momentum, and energy. In some cases it is impossible to conserve all these quantities. In these cases, CTH has been designed with several options that the sophisticated user can use to bound the effects.

Special emphasis has been placed on post-processing. The only efficient method of analyzing the results of a large three-dimensional calculation is with sophisticated graphics. Development of sophisticated graphical post-processing tools has been an ongoing part of the CTH project.

Section Two discusses the mesh and variable location. The solution scheme is described in Section Three. Section Four discusses the Lagrangian step. Section Five describes the remap step. The cell thermodynamics is discussed in Section Six. Post processing is described in Section Seven. Example calculations are discussed in Reference [1].

Eulerian Mesh and Variable Positions

The mesh is generated from three sets of spatial coordinates $x(i)$, $y(j)$, and $z(k)$, see Figure 1. The cell with logical coordinates (i,j,k) has spatial coordinates: $x(i) \leq x < x(i+1)$, $y(j) \leq y < y(j+1)$, $z(k) \leq z < z(k+1)$. In three dimensions, each computational cell is a rectangular parallelepiped (box). Two-dimensional and one-dimensional meshes are subcases of the three dimensional mesh.

All quantities are cell centered except the velocities, see Figure 2. All cell centered quantities are assumed to be uniform across the cell. The velocity is centered on a cell face and is perpendicular to the cell face. An auxiliary staggered mesh is constructed for the momentum conservation equation, see Figure 3. The velocity is assumed to be centered in the staggered cell and uniform across the staggered cell. The staggered cell boundaries coincide with the midpoints of the adjacent cells. The mass of the

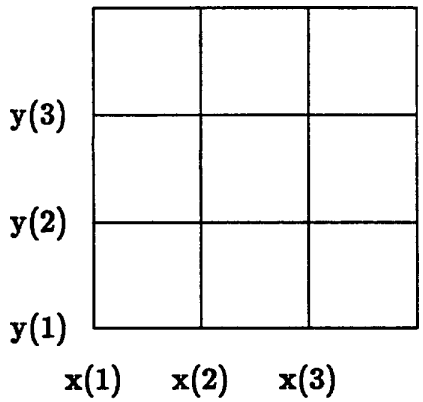

Figure 1: Eulerian Mesh

staggered cell is one half the mass of the two adjacent cells. These two assumptions are not consistent for cylindrical or spherical meshes. In particular, the mass is not a linear function of radius. The influence of this inconsistency has not been systematically examined. All quantities are temporally positioned at the timestep except the velocities which are at the middle of the timestep.

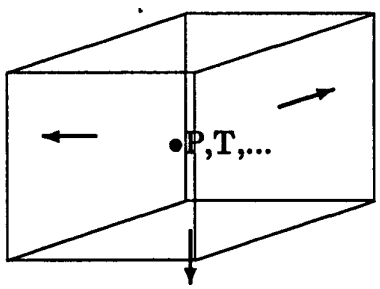

Figure 2: Cell Variable Positions

In the following text, it will be necessary to reference the mesh variables. The mesh variables will have four indices: timestep number (n), x coordinate index (i), y coordinate index (j), and z coordinate index (k). In some cases the y and/or z coordinate indices will be dropped for simplicity. The integer values of the indices are associated with the cell boundaries, refer to Figure 3. The pressure is centered in the cell, refer Figure 2, so all its spatial indices will have 'half' integer values. The pressure for the i,j,k-th cell is

$$P(n, i+\frac{1}{2}, j+\frac{1}{2}, k+\frac{1}{2}). \tag{1}$$

The x-velocity for the i,j,k-th cells is positioned in the center of the cell face, refer to

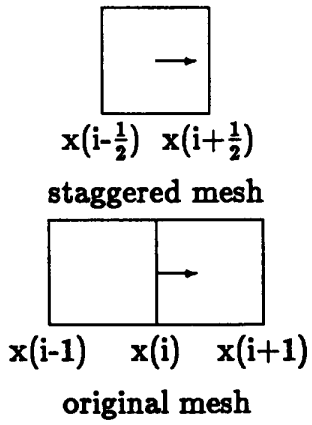

Figure 3: Original and Staggered Mesh

Figure 3, and is

$$v_x(n-\frac{1}{2}, i, j+\frac{1}{2}, k+\frac{1}{2}). \tag{2}$$

Solution Scheme

As mentioned above, CTH uses an Eulerian mesh that is fixed in space, and the material flows through the mesh. The Eulerian forms of the governing equations are solved in two steps: a Lagrangian step and a remap step. In the Lagrangian step, the Lagrangian forms of the governing equations are integrated across the timestep. The mesh distorts to follow the material motion and there is no mass flux across the cell boundaries. At the end of the Lagrangian step, the remap step is performed. In this step, the distorted cells are remapped back to the Eulerian mesh. The two step process is easy to develop and understand. It also makes handling multiple materials much easier.

Lagrangian Step

The conservation of volume, mass, momentum, and energy must be satisfied across the Lagrangian step. The conservation equations are replaced with explicit finite-volume equations. The explicit equations are easy to solve but they require a timestep that is sufficiently small so that a wave cannot cross a cell in one timestep. The timestep used is the minimum of the one derived by Hicks [3] and another that limits the volume change of a cell. The limit on the volume change prevents excessive compression or expansion of a cell.

The new volume is calculated from the old cell volume, cell face areas, and velocities. Since the same areas and velocities are used for adjacent cells, volume is conserved. There is no mass flux during the Lagrangian step so conservation of mass is trivially satisfied. An explicit finite volume approximation to the conservation of momentum is written for the staggered cell. The two-dimensional rectangular geometry form of the

finite volume equation is

$$
\begin{aligned}
v_x(n+\frac{1}{2},i,j+\frac{1}{2}) \;=\; & v_x(n-\frac{1}{2},i,j+\frac{1}{2}) + \\
& \Delta t(n)\{V(n,i+\frac{1}{2},j+\frac{1}{2}) + V(n,i-\frac{1}{2},j+\frac{1}{2})\} \\
& \{2\frac{\sigma^d_{xx}(n,i+\frac{1}{2},j+\frac{1}{2}) - \sigma^d_{xx}(n,i-\frac{1}{2},j+\frac{1}{2}))}{x(i+1)-x(i-1)} \\
& +\frac{\sigma^d_{xy}(n,i,j+1) - \sigma^d_{xy}(n,i,j)}{y(j+1)-y(j)}\}/ \\
& \{M(n,i+\frac{1}{2},j+\frac{1}{2}) + M(n,i-\frac{1}{2},j+\frac{1}{2})\},
\end{aligned}
\tag{3}
$$

where $\mathbf{v}$ is the velocity, $\Delta t(n) = (t(n+1) - t(n-1))/2$, V is the cell volume, $\sigma^{\mathbf{d}}$ is the stress deviator tensor, and M is the cell mass. Equation 3 is in conservative form so the total momentum of the calculation is conserved. The shear stress (σ^d_{xy}) appearing in Equation 3 is positioned on the cell corner rather than the cell center. It is interpolated from the four neighboring cells. The equation for the corner positioned shear stress is

$$
\begin{aligned}
\sigma^d_{xy}(n,i,j) \;=\; & \frac{1}{4}\{\sigma^d_{xy}(n,i-\frac{1}{2},j-\frac{1}{2}) + \sigma^d_{xy}(n,i-\frac{1}{2},j+\frac{1}{2}) \\
& +\sigma^d_{xy}(n,i+\frac{1}{2},j-\frac{1}{2}) + \sigma^d_{xy}(n,i+\frac{1}{2},j+\frac{1}{2})\}.
\end{aligned}
\tag{4}
$$

The conservation of energy equation for the Lagrangian step is rewritten as an evolution equation for the internal energy [2]. This is done using the conservation of energy, mass, and momentum equations. The resulting equation is

$$
\frac{d}{dt}\int_V \rho\varepsilon\, dV = -\int_S trace\{(P\mathbf{I} - \sigma^{\mathbf{d}})\cdot \mathbf{d}\}\, dS + \int_V Q\, dV, \tag{5}
$$

where V is the volume, ρ is the mass density, ε is the specific internal energy, S is the boundary of the volume, P is the pressure, $\mathbf{I}$ is the identity tensor, $\sigma^{\mathbf{d}}$ is the stress deviator tensor, $\mathbf{d}$ is the rate of stretching tensor, and Q is the energy source. The equation for the rate of stretching tensor is

$$
\mathbf{d} = \frac{1}{2}(\nabla\mathbf{v} + \mathbf{v}\nabla), \tag{6}
$$

where ∇ is the gradient operator, and $\mathbf{v}$ is the velocity vector.

Equations 5 is replaced with an explicit finite-volume approximation. The solution to the finite-volume approximation to Equation 5 will not conserve total energy unless a special form is used for the mechanical power. The mechanical power term is the first integral on the right hand side of Equation 5. The special form for the mechanical power

equation is derived from the momentum balance finite-volume equation. The equation for the mechanical power equation for a hydrodynamic material in one dimension is

$$\begin{aligned}\int_S trace(P\mathbf{I}\cdot\mathrm{d})\,dS &= \Delta t(n)\,P(n,i+\frac{1}{2}) \\ &\{A(i+1)(v(n-\frac{1}{2},i+1)+v(n+\frac{1}{2},i+1)) \\ &-A(i)(v(n-\frac{1}{2},i)+v(n+\frac{1}{2},i))\}/2,\end{aligned} \tag{7}$$

where $\int_S trace(P\mathbf{I}\cdot\mathrm{d})\,dS$ is the mechanical power, $\Delta t(n) = (t(n+1)-t(n-1))/2$, P is the pressure, A is the cell face area, and $\mathbf{v}$ is the velocity. Equivalent equations for multiple dimensions, curvilinear coordinates, and full stress tensors are straightforward but complicated to derive.

The mechanical power arises from three contributions: material pressure, artificial viscosity, and stress deviators. The mechanical power arising from the stress deviators is partititioned proportional to volume among the cell materials that can support shear. For example, the power in a cell containing metal and air would be deposited in the metal. The mechanical power arising from the pressure and artificial viscosity is partitioned among the cell materials according to their mass fraction.

CTH updates the value of the stress deviators using an incremental law. Two of the components of the rate law are

$$\frac{d\sigma^d_{xx}}{dt} = 2\{G(\frac{\partial v_x}{\partial x}-\frac{1}{3}\nabla\cdot\mathbf{v})+\omega_y\sigma^d_{xz}-\omega_z\sigma^d_{yz}\}, \tag{8}$$

and

$$\frac{d\sigma^d_{xy}}{dt} = 2\{G(\frac{\partial v_y}{\partial x}-\frac{\partial v_x}{\partial y})+\omega_z(\sigma^d_{xz}-\sigma^d_{yy})+\omega_y\sigma^d_{xy}-\omega_z\sigma^d_{xz}\}, \tag{9}$$

where G is the shear modulus, $\mathbf{v}$ is the velocity, ∇ is the gradient operator, and ω is the vorticity vector.

Two yield surfaces are currently available: a von Mises yield surface and a pressure dependent yield surface. Both surfaces limit the second invariant of the stress deviator. The pressure dependent yield surface has a low strength at low pressure, increasing strength as the pressure increases, and asymptotically approaches a von Mises surface at high pressures. The user can also include the effect of thermal softening. The flow rule associated with the von Mises yield surface is used for both yield surfaces. The shear modulus, Poisson's ratio, and yield strength for a multi-material cell is defined as the volume fraction weighted sum of the component materials.

Artificial viscosity is used to model shocks. A vector form for an artificial viscosity is used. In particular, the xx, yy, and zz components of the viscosity tensor are the only nonzero components. The viscosity uses both a linear and quadratic term.

High explosive detonation can be simulated using a programmed burn model and the Jones-Wilkens-Lee equation of state [4]. A special algorithm is used to determine the initiation time for each cell. The user specifies an initiation time, initiation point, and an exact burn region. Inside the exact burn region, the burn path is assumed to be a straight line. A less accurate finite difference scheme is used outside the exact burn region. Outside the exact burn region, a 27 cell cube (3 x 3 x 3 cells) containing at least one cell with a defined initiation time is considered. If the central cell contains no high explosive, then the next cube is considered. If the central cell does contain high explosive, then the detonation time of all cells will be calculated from the information available in the cube. The earliest of all calculated detonation times is used. This scheme requires multiple sweeps through the mesh but will define reasonably accurate burn times for very complicated geometries.

The velocities, energies, and stress deviators have been updated by the end of the Lagrangian step and must be remapped back to the mesh with the remap step. Significant computational time can be saved if it is noted that only some of the thermodynamic variables are required for the following remap step. Only the material energy, volume fraction, and mass is required for each material in a cell. Variables such as pressure and temperature are not required by the remap step. The required variables can be calculated for full, single-material cells that will not fracture without calling the cell thermodynamics routines. Depending on the cell thermodynamics used, it may be necessary to call the cell thermodynamics routines for multi-material cells, partially-full cells, and cells that might fracture.

Remap Step

The remap step remaps the deformed cells back to the original mesh. To do this, the appropriate amounts of volume, mass, momentum, and energy must be moved between the cells. First the volume flux between cells is calculated. Next the interface tracker algorithm decides which materials in the donor cell are moved with the volume. Then each material's mass and internal energy is moved between cells. Finally, the momentum and kinetic energy is moved between cells.

The remap differential equations are multidimensional and difficult to solve. They are simplified by using operator splitting techniques to replace the multidimensional equations with a set of one-dimensional equations. The remap scheme uses a second order accurate, conservative van Leer scheme [5,6] to improve the accuracy. The Van Leer scheme used in CTH replaces a uniform distribution in the donor cell with a linear distribution. This dramatically reduces numerical dispersion. Asymmetry can arise from the operator splitting, but it is minimized by permuting the order of the one-dimensional remaps. Using multiple one-dimensional passes also facilitates corner coupling between cells. Corner coupling occurs when two cells that share only a corner interact. For example, in two dimensions the cells with indices i,j and i+1,j+1 are neighbors, do share a corner, but do not share a side, refer to Figure 1. Corner coupling

is very important for modelling phenomena with motion skew to the mesh direction.

Once the volume flux across a cell face has been calculated, the volume of the materials advected must be calculated. This is difficult for multi-material or partially full cells. Interface reconstruction techniques are used to dynamically construct the material interfaces in a cell. These techniques are basically pattern matching algorithms that look at the neighboring cells and infer the material interfaces. The SLIC [7] scheme is available for all geometry options. A high-resolution interface tracker has been developed for two-dimensional meshes that gives much better resolution of material interfaces.

The two-dimensional, high-resolution interface tracker assumes the interface between two materials can be adequately approximated by a straight line, refer to Figure 4. The scheme calculates a volume fraction for each cell corner by averaging the material volume fractions of the four surrounding cells. The values in Figure 4 are .05, .8, .05, and .3. Values along the cell sides are defined by linearly interpolating the corner values. The .5 values on the right and bottom sides of Figure 4 are obtained by interpolating the corner values. The set of all possible material interfaces is generated from the interpolated values on the sides. This is done by connecting two points on different sides that have equal values. One possible interface line in Figure 4, connects the .5 values on the right and bottom sides. The volume below the line defines the volume associated with the line. For example, the volume associated with the line in Figure 4 is 12% of the cell volume. The line used is the one whose volume is equal to the material volume. Once the geometry of the material volume is determined, the intersection of the volume flux and the material volume is the material moved across the boundary. For example, in Figure 4 the volume to the right of the dashed line is the volume flux. The intersection of the volume flux and the material volume is the volume of the material moving across the boundary. In the case of Figure 4 approximately 40% of the material volume is fluxed through the right side.

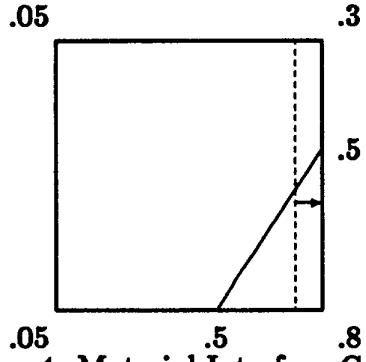

Figure 4: Material Interface Construction

An interesting and difficult problem arose in several calculations with large compressions. The fluxed volume, mass, and energy were known, so it was possible to calculate

an average mass density and an average specific internal energy of the fluxed materials. From these average variables, it was possible to calculate an average temperature of the fluxed material. The temperature was often much higher or lower than the donor or acceptor cells. Severe temperature fluctuations were observed in both the donor and acceptor cells. This difficulty was solved by coupling the mass and energy convection. The original van Leer scheme assumed that density was a linear function of volume and the internal energy was a linear function of mass. The new scheme makes no change in the density distribution, but it assumes the internal energy is a linear function of density, refer to Figure 5. The slope is calculated from the internal energies and densities of the neighboring cells. With the new scheme, the density as a function of volume is known, and the internal energy as a function of density is known, so the mass and energy flux can be calculated. This modification solved the problem. It should be noted that this problem will occur only with internal energies that are a strong function of mass density. This problem will not be observed with ideal gasses.

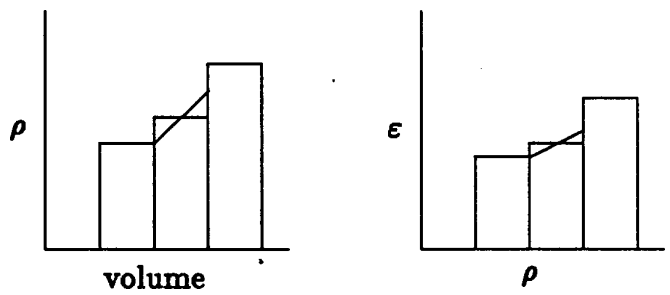

Figure 5: Density and Internal Energy Advection Profiles

The mass, momentum and kinetic energy cannot be conserved across a remap. All three quantities are calculated from the two database variables mass and velocity. Three options for rezoning the momentum and kinetic energy are available for the analyst. In the first, the momentum is conserved and the kinetic energy discrepancy is transformed into an internal energy source or sink. This scheme conserves the total energy in a calculation but often overheats a material. In the second scheme, the kinetic energy is conserved but the momentum is not. The amplitude of the velocity is calculated from the kinetic energy and the sign is inferred from the momentum. This conserves the total energy but does not seem to give the best answers. In the third scheme, the momentum is conserved and the kinetic energy discrepancy is discarded in all cases except one. If the momentum fluxed into an acceptor cell has the opposite sign as the acceptor cell's momentum, then the kinetic energy discrepancy is deposited in the internal energy. This energy source is conceptually like an inelastic collision between two bodies. The third scheme seems to give the best answers and is most commonly used by the analysts. Analysts can run with all three options to examine the influence of this numerical error.

Isolated objects smaller than a cell do not move through the mesh at the correct velocity. They tend to stop moving while the surrounding fluid rushes by. This is because the interface tracker does not know where to position a small fragment and it cannot determine if the fragment is fluxed across a cell boundary. For example, is the material at the top or bottom of the cell? CTH uses a random number to specify the location of the fragment's center of mass. Once the location of the center of mass is known, it is easy to determine if part or all of the fragment is swept across the boundary. With this model, fragments move through the mesh with statistically the correct velocity. This model can generate some undesirable side effects. It is possible for fragments to 'tunnel' through plates or walls and emerge on the other side. The analyst can disable this model for materials that are not expected to fragment, such as gases.

Cell Thermodynamics

Strong shock calculations require accurate thermodynamic models. Phase changes, chemical changes, nonlinear behavior, and fracture all play important roles. CTH uses tabular or analytic [8] equations of state that are functions of mass density and temperature. The analytic equation of state uses a Helmholtz potential to calculate the thermodynamic quantities. This assures consistency between the thermodynamic quantities. Each material can be solid, liquid, vapor, or mixed-phase. Liquid-vapor, liquid-solid, and solid-solid phase transitions are modelled. The equations of state are defined for all temperatures and densities encountered in shock calculations.

Tensile states and fracture in solids are modelled. Crack formation is simulated when the principle stress or pressure drops below a user-specified value. The stress state is relaxed by introducing void in the cell over a several computational cycles. This increases the density and raises the pressure.

Each computational cell contains one or more materials and may contain void. The thermodynamic state of the cell must be determined from the volume, energy, and mass of each material. When only one material occupies the cell, the mass density is known and the temperature is chosen to conserve the energy.

The thermodynamics of multi-material cells is much more complicated. Three thermodynamic models are currently available. In all the models each material occupies a separate region of space like a mixture of oil and water, rather than occupying the same volume like a mixture of ideal gases.

The first thermodynamic model assumes all materials are at the same temperature and pressure. The governing equations are complex nonlinear algebraic equations that are solved with a multi-variable Newton's iteration. This model exhibits an unrealistic energy flow from a hot material to a cold material. Also, solid material in a cell containing vapor will not fracture because the pressure in the vapor cannot go into tension. Non-unique solutions will occur if two materials have identical equations of state and simultaneously go into mixed-phase thermodynamic regions.

The second model allows each material to have a different temperature but all have the same pressure. The model proceeds as follows: The mechanical power is partitioned between the materials according to volume fraction. The initial divergence of each material is equal to the cell divergence. An effective pressure is calculated from the mechanical power and the volume change. The equation for the effective pressure (P_{eff}) is

$$P_{eff} = \frac{Mechanical\ Power}{Cell\ Volume\ Change}. \tag{10}$$

The volume of each material is adjusted until all materials are at the same pressure. The effective pressure is used when calculating the PdV work of one material on another. This scheme has the property of partitioning the mechanical power proportional to the material's volume change. For example, if one material was very stiff, the second was very soft, and the stiff material did not change volume, then all the mechanical power would be deposited in the soft material. A set of springs in series is a good mechanical analog for this model. If this model fails to converge, then the single temperature, single pressure model is used.

This model is superior to the first but can generate poor answers in some situations. For instance, solid material in a cell containing vapor will not fracture because the pressure in the vapor cannot go into tension. Another problem arises when a rapidly-moving cell containing solid and vapor stagnates. When this happens, the kinetic energy is transformed into internal energy. The equal pressure assumption results in a volume change in the solid that is much smaller than that of the vapor. Therefore, most of the cell's kinetic energy is converted into internal energy in the vapor. This can cause the vapor to heat up to unrealistic values.

In the third model each material has a different temperature and pressure. This model partitions the mechanical power proportional to mass fraction. It assumes the divergence of each material is equal to the divergence of the cell. It allows no change in the volume and no coupling between materials. The cell pressure is the volume fraction weighted average of the material pressures. A set of springs in parallel is a good mechanical analog for this model. This model gives surprisingly good answers. However, the current implementation of this model contains no mechanism that allow the pressures to relax to an equilibrium value. If the energy of a material drops below a threshold value, then the single pressure, multiple temperature model is used for this cell. This model is still under development and testing.

Post-Processing

CTHED is the interactive post-processing program for CTH. It is principally used to generate three-dimensional color shaded plots of the material configurations. The analyst can specify the colors used for the materials, specify the materials plotted, specify the region plotted, and apply several filters to the materials plotted. The filters remove material with properties that fall outside user specified ranges. The filters can

be applied to the temperature, pressure, mass density, and velocity. For example, this allows the analyst to filter out vapor or cold material. The three-dimensional plots are the principle tool for analysis of calculations and for explaining the calculation results to the customer.

CTHED can also generate two-dimensional color plots using a modified version of the CSQII post-processing code CSQPLT [9]. The two-dimensional plane must be an x-y, y-z, or x-z plane. A very large number of options are available including color band plots, material shading, dot density, and contour plots.

CTHED can also generate edits in a variety of formats. The edits can range from interactive edits of individual cell data, to line-printer plots, to enormous line-printer edits for three-dimensional calculations.

References

Hicks, D. L., "von Neumann Stability of the Wondy Wavecode for Thermodynamic Equations of State," Sandia National Report SAND-77-0934, Sandia National Laboratories, Albuquerque, NM, 1977.

McGlaun, J. M., "Improvements in CSQII: An Improved Numerical Convection Algorithm," Sandia National Laboratories Report SAND82-0051 Sandia National Laboratories, Albuquerque, NM, January 1982.

Noh, W. F., and P. Woodward, "SLIC (Simple Line Interface Calculation)," in Proc. of the Fifth International Conference on Numerical Methods in Fluid Dynamics, Springer Lecture Notes in Physics vol 59, 1976, pp 330-340.

Rottler, J. S. and S. L. Thompson, "CSQPLT: A Graphics Post Processor for Multidimensional Wave Propagation Codes," Sandia National Laboratories Report SAND87-2018, Sandia National Laboratories, Albuquerque, NM, November, 1987.

Thompson, S. L., "Improvements in the Chart D Radiation-Hydrodynamic CODE V: 1972/1973 Modifications," Sandia National Report SLA-73-0477, Sandia National Laboratories, Albuquerque, NM, October, 1973.

Thompson, S. L. and H. S. Lauson, "Improvements in the Chart D Radiation-Hydrodynamic CODE III: Revised Analytic Equations of State," Sandia National Report SC-RR-71 0714, Sandia National Laboratories, Albuquerque, NM, March 1972.

Trucano, T. G. and J. M. McGlaun, "Hypervelocity Impact Computation with CSQIII and CTH," These proceedings.

Truesdell, C. and R. A. Toupin, "The Classical Field Theories," in Encyclopedia of Physics, Vol III/1, Ed: S. Flugge, Springer Verlag, Berlin, 1960.

van Leer, B., "Towards the Ultimate Conservative Difference Scheme IV. A New Approach to Numerical Convection," J. Comp. Phys. 23, 276-299, 1977.

DISCLAIMER